

# Proliferation and Remodeling of the Peritubular Microcirculation after Nephron Reduction

## *Association with the Progression of Renal Lesions*

Evangéline Pillebout,\* Martine Burtin,\*  
Hai T. Yuan,<sup>†</sup> Pascale Briand,<sup>‡</sup> Adrian S. Woolf,<sup>†</sup>  
Gérard Friedlander,\* and Fabiola Terzi\*

From INSERM U426,\* Faculté de Médecine Xavier Bichat, Université Paris, Paris, France; INSERM U380,<sup>‡</sup> Institut Cochin de Génétique Moléculaire, Paris, France; and the Nephro-Urology Unit,<sup>†</sup> Institute of Child Health, University College London, London, United Kingdom

**Little is known about the serial changes that might occur in renal capillaries after reduction of renal mass. In the current study, our aim was to document potential alterations in the morphology and proliferation of the renal cortical peritubular microcirculation at specific time points (7 and 60 days) after experimental 75% surgical nephron reduction using two strains of mice that we here demonstrate react differently to the same initial insult: one strain (C57BL6xDBA2/F1 mice) undergoes compensatory growth alone, whereas the other (FVB/N mice) additionally develops severe tubulo-interstitial lesions. Our data demonstrate that significant remodeling and proliferation occur in renal cortical peritubular capillaries after experimental nephron reduction, as assessed by microangiography using infusion of fluorescein isothiocyanate-labeled dextran, expression of the endothelial markers CD34 and Tie-2, and co-expression of CD34 and proliferating cell nuclear antigen, a surrogate marker of cell proliferation. This was accompanied by an increase of renal vascular endothelial growth factor protein levels and a change in distribution of this protein within the kidney itself. Moreover, most of these responses were accentuated in FVB/N mice in the presence of progressive renal disease and positively correlated with tubular epithelial cell proliferation. Hence, we have made three significant novel observations that illuminate the complex pathophysiology of chronic kidney damage after nephron reduction: 1) cortical peritubular capillaries grow by proliferation and remodeling, 2) vascular endothelial growth factor expression is altered, and 3) the development of tubulo-interstitial disease is genetically determined. (*Am J Pathol* 2001, 159:547–560)**

Reduction of renal mass triggers molecular and cellular events promoting compensatory growth of remaining nephrons. In some cases, the compensatory process becomes pathological with the development of glomerulosclerosis, tubular cyst formation, interstitial fibrosis, and end-stage renal failure.<sup>1</sup> Although the pathophysiology of compensation and progression is certain to be highly complex, the proliferation of glomerular, tubular, and interstitial cells has been implicated in the pathogenesis of progressive kidney lesions.<sup>2–5</sup> Indeed, the reduction of renal cell proliferation by inhibition of growth factors using pharmacological inhibitors,<sup>6</sup> neutralizing antibodies,<sup>7</sup> antisense nucleotides,<sup>8</sup> or a dominant-negative transgenic strategy<sup>9</sup> reduces the progression of renal lesions in some experimental models of injury.

In contrast to the relatively well-established changes in epithelia and interstitial cells, described above, less is known about the serial changes that might occur in renal capillaries after reduction of renal mass. In an experimental unilateral nephrectomy model, rat glomerular capillary expansion, as assessed by the presence of giant capillary loops, was reported at 12 weeks after surgery.<sup>10</sup> By contrast, a study of subtotal nephrectomized rats reported a net decrease of glomerular endothelial cells between 3 to 6 months after surgery, and the same study provided evidence that these cells were deleted by apoptosis.<sup>11</sup> Similarly, Ohashi and colleagues,<sup>12</sup> using a rat model of experimental glomerulonephritis that was followed by tubulo-interstitial scarring, reported loss of peritubular capillaries mediated, at least in part, by apoptosis. Other investigators have attempted to assess the response of renal capillaries in humans with chronic renal failure associated with a variety of primary insults.<sup>13–15</sup> For example, Seron and colleagues<sup>13</sup> assessed peritubular capillary cross-sections per area using two endothelial antibodies and reported that this parameter was reduced in patients *versus* normals and correlated with

---

Supported by INSERM, Université René Descartes, Laboratoires de Recherches Physiologiques, Association pour la Recherche contre le Cancer (project grant no. 9896), CEGETEL Company, CRIT Company, Wellcome Trust (project grant no. 058008), and the Kidney Research Aid Fund.

Accepted for publication April 19, 2001.

Address reprint requests to Fabiola Terzi, INSERM U426, Faculté de Médecine Xavier Bichat, 16, Rue Henri Huchard, BP 416, 75870 Paris, Cedex 18, France. E-mail terzi@cochin.inserm.fr.

the degree of interstitial damage and reduction of whole kidney glomerular filtration rate. In a review, Bohle and colleagues<sup>14</sup> presented evidence that there was a paucity of vessels in various human glomerulonephritis and interstitial diseases based on measuring the number and area of intertubular capillaries. In contrast, a recent detailed study by Konda and colleagues,<sup>15</sup> using CD34 as an endothelial marker, demonstrated that the microvessel count actually increased with increasing interstitial fibrosis in scarred kidneys from patients with lower urinary tract disease. Furthermore, immunostaining for endogrin, a marker of endothelial proliferation, increased in microvessels located in the fibrotic interstitium.<sup>15</sup> However, we are not aware of any study of either experimental animals or humans that has systematically documented the serial changes in the cortical peritubular microcirculation after nephron reduction associated with either compensatory growth alone or with the additional development of progressive tubulo-interstitial lesions.

Capillary growth is mediated by a complex balance of positive and negative soluble factors as well as cell-cell and cell-matrix interactions.<sup>16</sup> Among these regulators, vascular endothelial growth factor (VEGF) plays a key role. Indeed, VEGF induces a pleiotropic endothelial response involving proliferation, differentiation, migration, and assembly into tubes.<sup>17</sup> During kidney development, VEGF is critical for capillary growth.<sup>18</sup> In the normal adult kidney, VEGF is expressed by podocytes and by tubular epithelia,<sup>19</sup> but its role in the healthy mature organ is unclear. More recent evidence suggests that other growth factors mediate endothelial growth. These include the angiopoietins, which bind the Tie-2 receptor, and this signaling system is also expressed in the kidney and is developmentally regulated.<sup>20</sup>

In the current study, our aim was to document potential alterations in the morphology and proliferation of the renal cortical peritubular microcirculation at specific time points (7 and 60 days) after experimental 75% surgical nephron reduction using two strains of mice that we here demonstrate react differently to the same initial insult: one strain (C57BL6xDBA2/F1 mice) undergoes compensatory growth alone, whereas the other (FVB/N mice) additionally develops severe tubulo-interstitial lesions. Our data clearly demonstrate that significant remodeling and proliferation occur in renal cortical peritubular capillaries after experimental nephron reduction, as assessed by microangiography and expression of the endothelial markers CD34 and Tie-2. This is accompanied by an increase of renal VEGF protein levels and a change in distribution of this factor within the kidney itself. Moreover, these responses were accentuated in the presence of progressive renal disease and positively correlated with tubular epithelial proliferation, suggesting an association between vessel growth and renal deterioration.

## Materials and Methods

### Animals

All experiments were performed on 9-week-old female mice from C57BL6×DBA2/F1 (B6D2F1) and FVB/N (FVB)

strains (Iffa Credo, Fresnes, France). Animals were fed *ad libitum*, and housed in a room with constant ambient temperature and a 12-hour light-dark cycle. All animal procedures were conducted in accordance with French government policies (Services Vétérinaires de la Santé et de la Production Animale, Ministère de l'Agriculture).

### Experimental Protocol

Surgery was performed under xylazine (Rompun 2%; Bayer, Leverkusen, France) (6  $\mu$ g/g of body weight) and ketamine (Clorketam 1000; Vetoquinol SA, Lirre, France) (120  $\mu$ g/g of body weight) anesthesia. Subtotal nephrectomy (Nx) was performed as previously described.<sup>21</sup> Briefly, the right kidney was removed and the two poles of the left kidney were excised to reach 75% reduction of total renal mass, on 24 mice of each strain. Sham control mice (Sh;  $n = 24$  in each strain) were subjected to decapsulation of both kidneys. After surgery, mice were fed a defined diet containing 20% (w/w) casein and 0.5% sodium. Previous experiments have shown that the sodium content of this diet favors the development of renal lesions in 70% nephrectomized rats.<sup>22</sup> Mice from the four groups (B6D2F1-Sh, B6D2F1-Nx, FVB-Sh, FVB-Nx) were sacrificed at 7 and 60 days after surgery. Our preliminary studies (data not shown) had demonstrated that these time points spanned a period of compensatory growth in both strains and, in the FVB strain, the progression of renal lesions; the operated FVB mice began to have significant mortality in the third month, precluding analysis of further times. At each time point, mice were matched for body weight and kidneys were removed, weighed, and analyzed by Northern blot and immunohistochemistry ( $n = 6$  in each group) or by Western blot and morphological studies ( $n = 6$  in each group). Before sacrifice, six mice of each group underwent microangiography, as described below. Finally, to determine whether differences in renal morphology as well as in renal microcirculation existed between the two mouse strains under physiological conditions, six normal nonoperated mice of each strain were also studied.

### Microangiography

Mice were subjected to intrajugular injection of fluorescein isothiocyanate-dextran (ICN Biomedicals Inc., Orsay, France) (100  $\mu$ g/g of body weight) in isotonic saline. Four minutes after injection, mice were sacrificed and kidneys were removed and immediately fixed in 4% formalin overnight, ethanol-dehydrated, and paraffin-embedded. Preliminary experiments demonstrated that this delay between injection and sacrifice is optimal to detect fluorescence in renal vessels (data not shown). Four- $\mu$ m-thick sections were cut, counterstained, and mounted with 4,6-diamidino-2-phenylindole (Vectashield; Vector Biosys SA, Compiègne, France). Sections were then imaged with a Microphot-Fxa microscope (Nikon Eclipse E 800; Nikon, Champigny sur Marne, France) at  $\lambda = 515$  to 555 nm.

## *Histology and Immunohistochemistry*

Kidneys were fixed in 3.7% paraformaldehyde overnight at 4°C, ethanol dehydrated, and paraffin embedded. Four- $\mu\text{m}$ -thick sections were stained with periodic acid-Schiff. A pathologist, blinded to the nature of the group being examined, evaluated all sections.

### *CD34 and Tie-2 Immunostaining*

Six- $\mu\text{m}$  sections were trypsin-predigested (0.1 mg/ml; Sigma, Saint Quentin Fallavier, France) for 10 minutes at 37°C. Then, sections were incubated overnight at 4°C with a rat anti-mouse CD34 antibody (Pharmingen, Becton Dickinson, Le Pont de Claix, France) diluted 1/50 or with a rabbit anti-human Tie-2 antibody (Tebu, Santa Cruz, Le Perray en Yvelines, France) diluted 1/2000. Bound primary antibody was detected with a biotinylated rabbit anti-rat antibody (Vector) diluted 1/200 or a biotinylated anti-rabbit antibody followed by avidin/biotin/peroxidase system (strept ABCComplex HRP; DAKO, Trappes, France). 3-3'-Diaminobenzidine tetrahydrochloride (DAB, DAKO) was used as chromogen, and sections were counterstained with Meyer's hemalum and mounted in Eukitt (Labo Nord, Villeneuve d'Asq, France).

### *Proliferating Cell Nuclear Antigen (PCNA) Immunostaining*

Six- $\mu\text{m}$  sections were incubated overnight at 4°C with a mouse monoclonal anti-human PCNA antibody (DAKO) conjugated with peroxidase, diluted 1/20. Sections were then directly incubated with DAB, counterstained with Meyer's hemalum, and mounted in Eukitt.

### *CD34/PCNA Double Immunostaining*

Sections were first incubated with the mouse monoclonal anti-human PCNA antibody overnight at 4°C and stained with DAB. Then, sections were incubated with the rat anti-mouse CD34 antibody for 1 hour at room temperature and with the biotinylated rabbit anti-rat antibody, following the same procedure as described above, except for peroxidase activity that was detected using 3-amino-9-ethylcarbazole (DAKO). Finally, the sections were counterstained with Meyer's hemalum and mounted in glycerol gelatin (Merck Eurolab, Nogent sur Marne, France).

### *VEGF Immunostaining*

Six- $\mu\text{m}$  sections were incubated overnight at 4°C with a rabbit anti-human VEGF (Tebu, Santa Cruz) antibody diluted 1/100. Bound primary antibody was then detected with a biotinylated anti-rabbit antibody associated with an avidin/biotin/peroxidase system (LSAB2 kit, DAKO). 3-Amino-9-ethylcarbazole was used as chromogen. Sections were counterstained with Meyer's hemalum and mounted in glycerol gelatin (Merck Eurolab). To enhance glomerular VEGF stain-

ing, sections were processed by microwave for 10 minutes in citrate buffer (10 mmol/L, pH 6.0).

Negative controls were obtained by replacing specific antisera with normal nonimmune sera; no labeling was observed, indicating that all of the procedures and reagents used resulted in specific labeling.

To score immunostaining, a pathologist, blinded to the nature of the group being examined, evaluated all sections using a Microphot-Fxa microscope. To estimate the number of peritubular capillaries, we captured the images of immunostained sections using a Sony DXC-950P camera (Sony, Tokyo, Japan) fixed to the light microscope and printed the captured images on UPC-120 Sony paper. Counting was performed on the printed images. The number of CD34-labeled peritubular vessels was determined on five randomly selected fields ( $\times 200$  objective) from the cortex and factored for the number of tubular cross-sections of the same field. Both transverse and longitudinal capillary cross-sections were counted. The number of double PCNA/CD34-stained cells was determined on the whole cortex kidney ( $\times 400$ ) and factored for the number of fields. The number of PCNA-labeled tubular nuclei was determined in 10 randomly selected fields of the cortex ( $\times 200$ ) and factored for the number of tubular sections.

## *Western Blot*

Thirty  $\mu\text{g}$  of protein was fractionated on a sodium dodecyl sulfate-polyacrylamide gel (8% for CD34 and 12% for VEGF) and transferred to a nitrocellulose membrane (Bio-rad, Ivry sur Seine, France). The membrane was incubated, first 1 hour at room temperature with the primary antibody, then, for 1 hour at room temperature with the peroxidase-conjugated secondary antibody. Immunoreactive proteins were detected by enhanced chemiluminescence (ECL kit; Amersham Pharmacia, Les Ulis, France). Films were scanned using a Scan-Jet/ADF (Hewlett Packard, Canberra Company, Meriden, CT) and the signals quantified with NIH image software. The 5'-nucleotidase antibody was used to quantify protein loading on the gel and to compare the intensity of the hybridization obtained in the different lines. Indeed, it has been previously shown that 5'-nucleotidase protein level does not change after subtotal nephrectomy.<sup>23</sup>

## *Antibodies*

Primary antibodies used in the present study were: 1) a rat polyclonal anti-mouse CD34 (Pharmingen), diluted 1/2000; 2) a goat polyclonal anti-human VEGF (Santa Cruz), diluted 1/1500; 3) a rabbit polyclonal anti-rat 5'-nucleotidase (kindly provided by Dr. B. Kaissling, Anatomisches Institut der Universität, Zürich, Switzerland), diluted 1/6000. The secondary antibodies used in this study were: 1) a rabbit anti-rat horseradish peroxidase-linked Ig antibody (Amersham), diluted 1/200 for CD34; 2) a donkey anti-goat horseradish peroxidase-linked Ig antibody (Santa Cruz), diluted 1/10,000 for VEGF; 3) a

**Table 1.** Data at Sacrifice

	B6D2F1						FVB					
	Sh			Nx			Sh			Nx		
	BW (g)	KW (mg)	K/B (%)	BW (g)	KW (mg)	K/B (%)	BW (g)	KW (mg)	K/B (%)	BW (g)	KW (mg)	K/B (%)
Day 0												
Mean	20	128	0.63	21	70*	0.33*	23 <sup>§</sup>	126	0.55	23 <sup>§</sup>	70*	0.31*
SEM	0.2	2	0.005	0.4	2	0.006	0.3	5	0.018	0.4	1	0.060
Day 7												
Mean	21	132	0.63	18*	108*	0.59	24 <sup>§</sup>	132	0.56 <sup>†</sup>	20* <sup>‡</sup>	139 <sup>§</sup>	0.68* <sup>‡</sup>
SEM	0.2	3	0.012	0.2	3	0.018	0.5	3	0.010	0.5	6	0.022
Day 60												
Mean	24	143	0.61	23	131	0.58	27 <sup>§</sup>	148	0.54	25 <sup>‡</sup>	219* <sup>§</sup>	0.89* <sup>§</sup>
SEM	0.3	2	0.011	0.4	3	0.014	0.4	4	0.013	0.4	15	0.062

Sh, sham-operated mice; Nx, subtotaly nephrectomized mice; BW, body weight; KW, left kidney weight; K/B, left kidney weight/body weight. Data are mean ± SEM of 12 mice at each time. Analysis of variance: Nx versus Sh mice: \*,  $P < 0.001$ ; FVB versus B6D2F1 mice: <sup>†</sup> $P < 0.05$ ; <sup>‡</sup> $P < 0.01$ , <sup>§</sup> $P < 0.001$ .

donkey anti-rabbit horseradish peroxidase-linked Ig antibody (Amersham), diluted 1/8000 for 5'-nucleotidase.

### Northern Blot

Total RNA was extracted from whole kidneys using RNAzol kit (Bioprobe, Montreuil-sous-Bois, France). Twenty µg of total RNA was electrophoresed in 1% agarose-formaldehyde gel, transferred onto nylon membrane (Hybond-N, Amersham) and fixed by heat (2 hours at 80°C). Blots were prehybridized with Quick-Hyb solution (Stratagene, Saint Quentin en Yvelines, France) at 68°C for 20 minutes, and then hybridized with specific probes at 68°C for 1 hour. After hybridization the filters were washed according to the manufacturer's recommendations. RNA was quantified by densitometric computer analysis in a Packard Instant Imager. RNA extracts from heart were used as positive control.

### Probes

cDNA probes were labeled by the random priming method (Amersham) using [ $\alpha$ -<sup>32</sup>P]dCTP. The following probes were used: the human VEGF, the murine angiopoietins 1 and 2, and the murine glyceraldehyde-3-phosphate dehydrogenase (GAPDH) (kindly provided by Dr. E. Solito, Imperial College School of Medicine, London, UK). To generate VEGF probe, a fragment of human VEGF cDNA was amplified by reverse transcriptase and polymerase chain reaction using the following oligonucleotide primers (Gibco BRL, Cergy Pontoise, France): 5' oligonucleotide, 5'-d(CTGGACCCTGGCTTTACTGCT) and 3' oligonucleotide, 5'-d(GCACTCCAGGGCTTCAT-CATT). Plasmids with mouse angiopoietin-1 and angiopoietin-2 cDNA inserts have been described previously.<sup>20</sup> The GAPDH probe was used to quantify the RNA loading on the gel and to compare the intensity of hybridization obtained in the different lines.

### Expression of Data and Statistical Analysis

Data were expressed as means ± SEM. Differences between the experimental groups were evaluated using

one-way analysis of variance, which was followed, when significant, by the Bonferroni test.

## Results

### Evolution of Morphological Changes after Subtotal Nephrectomy

We performed 75% reduction of renal mass in two strains of 9-week-old mice, C57BL6xDBA2/F1 and FVB/N, and studied their remnant kidneys at 7 and 60 days after surgery. In addition, to compare response between strains, we also analyzed samples from sham-operated mice. In the sham-operated group, there was a small increase in body and wet-kidney weights of <15% during the 60-day period of observation, without changes in the kidney/body weight ratios (Table 1). By contrast, in nephrectomized mice, there was a marked and progressive increase in remnant wet-kidney weight (87 and 213% in C57BL6xDBA2/F1 and in FVB/N, respectively), whereas the increase of body weight was similar to that of sham-operated animals. The kidney weight increment was greater in FVB/N mice at each time point, and exceeded that of body weight, resulting in high kidney/body weight ratios (Table 1).

Figure 1 depicts histology of the experimental groups. In the sham-operated kidneys, we observed no gross differences of renal morphology in either strain during the course of the experiment; moreover, the appearance of the two strains was grossly similar (Figure 1, A and B). The histological appearance of remnant kidneys of C57BL6xDBA2/F1 mice revealed hypertrophy of tubules and glomeruli from day 7, but no pathological lesions such as glomerular sclerosis, tubular dilations, or interstitial fibrosis could be detected up to 60 days (Figure 1C). In FVB/N mice, compensatory growth of well-preserved tubules and glomeruli were also observed at 7 days but, in marked contrast to the C57BL6xDBA2/F1 strain, severe lesions were recorded at 60 days. These lesions were mainly comprised of severe tubular dilation with microcyst formation although sparse areas of interstitial fibrosis and mononuclear cell infiltration were

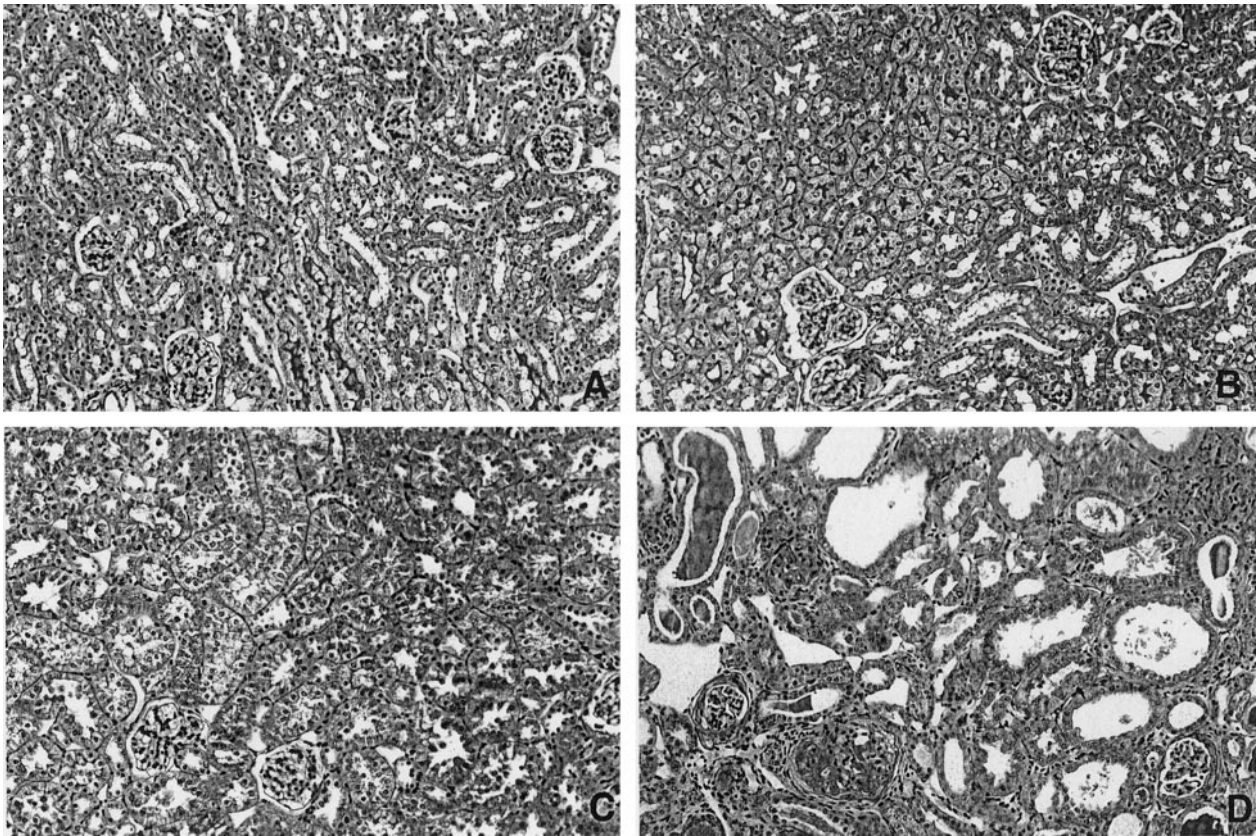


**Figure 1.** Morphology of sham-operated (A and B) and remnant (C and D) kidneys from B6D2F1 (A and C) and FVB (B and D) mice 60 days after surgery. Nephron reduction induced severe renal lesions in kidneys from FVB mice but not in those from B6D2F1 mice (compare C to D). Periodic acid-Schiff staining. Original magnification,  $\times 200$ .

noted. At this stage, glomerulosclerosis was present (Figure 1D).

### The Peritubular Microcirculation after Subtotal Nephrectomy

To obtain a measure of the total renal endothelial mass in the experimental groups, we quantified CD34-immunoreactive protein by Western blot. In sham-operated animals, at 7 days after surgery, CD34 protein levels were significantly higher in FVB/N mice compared to C57BL6xDBA2/F1 animals (Figure 2A). By contrast, no differences were observed between the two strains at day 60 (Figure 2B) as well as in control nonoperated mice (data not shown). At 7 days after nephron reduction, there was a significant increase in CD34/5'-Nu protein ratio in the remnant kidneys of both strains *versus* their sham-operated counterparts, and this response was greater in FVB/N *versus* C57BL6xDBA2/F1 mice. A similar pattern was recorded at the final time point of 60 days, but was only significant in FVB/N mice.

The above data are consistent with an increase of endothelial mass in the remnant kidney as a whole. To address whether changes had occurred in the cortical peritubular microcirculation we next performed immunohistochemistry for CD34. Figure 3 depicts photomicrographs at various time points and Figure 4 shows our quantitative grading of these appearances. At day 0, we

found CD34 immunoreactivity in both strains, predominantly in glomeruli and the vasa rectae, with faint staining in cortical peritubular capillaries (data not shown). A similar appearance was observed in sham-operated mice at days 7 and 60, with no difference between the two strains

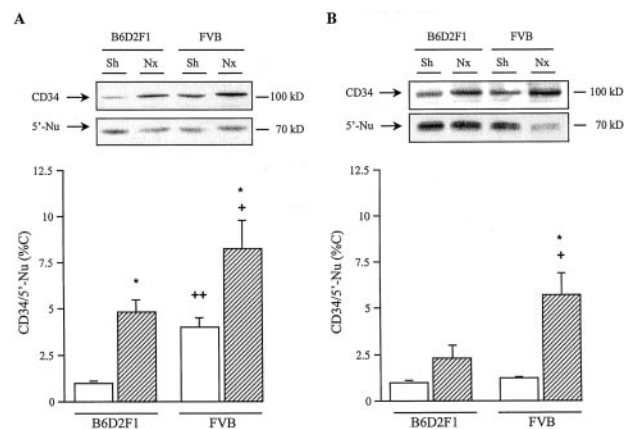


**Figure 2.** Western blot analysis of CD34 protein expression in sham-operated (open bars) and remnant (hatched bars) kidneys from B6D2F1 and FVB mice, 7 (A) and 60 (B) days after surgery. As compared to sham-operated mice, CD34 expression increased in remnant kidneys 7 days after nephron reduction, particularly in FVB mice (A). The increment was still greater in FVB-nephrectomized mice at day 60 (B). Blots are representative samples of six animals from each group. Data are means  $\pm$  SEM. Analysis of variance, followed by Bonferroni test (Nx *versus* Sh mice: \*,  $P < 0.05$ ; FVB *versus* B6D2F1 mice: +,  $P < 0.05$ ; ++,  $P < 0.01$ ).

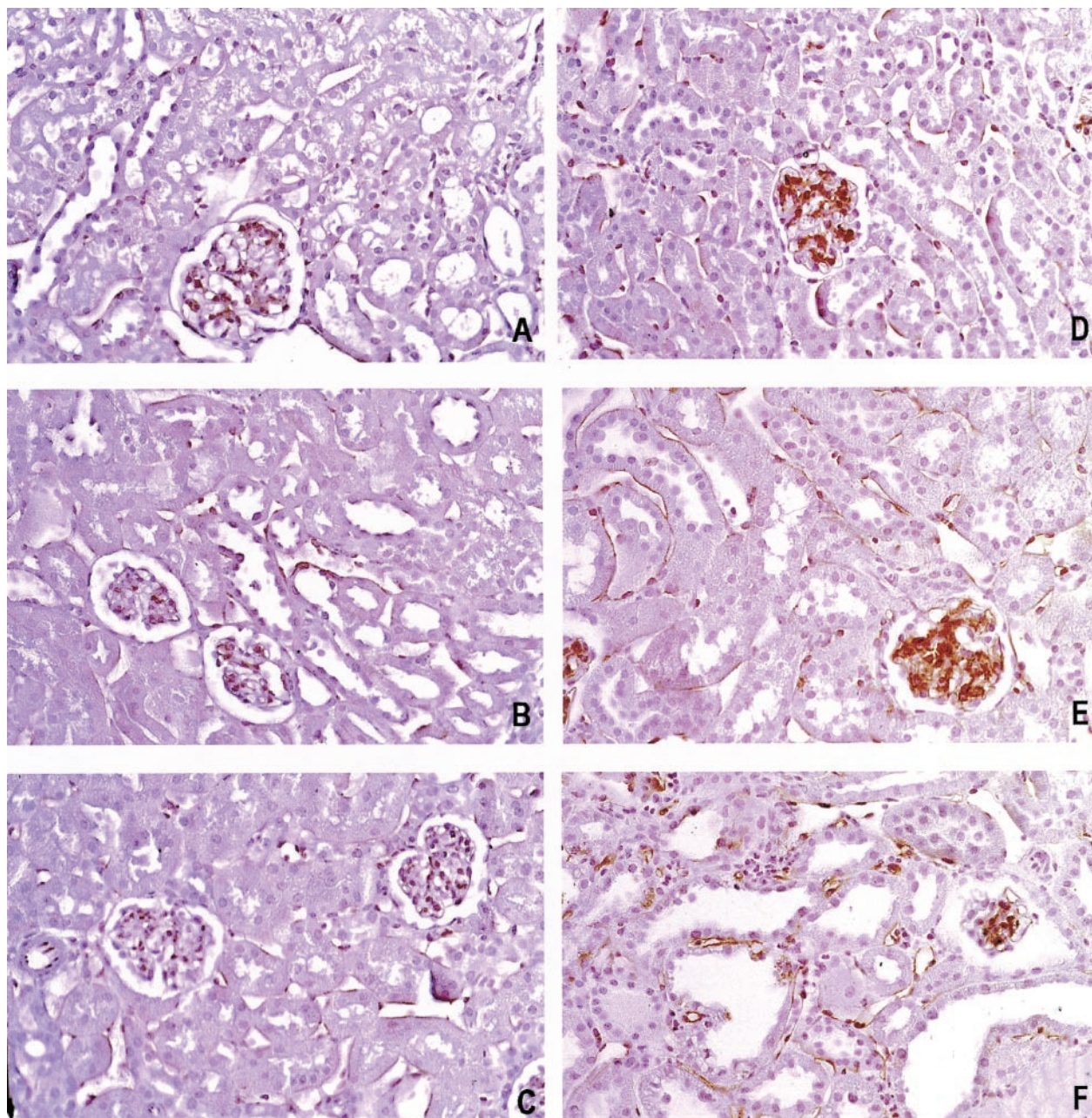


**Figure 3.** Immunohistochemical analysis of CD34 protein expression in cortex of sham-operated (**A** and **D**) and remnant (**B**, **C**, **E**, and **F**) kidneys from B6D2F1 (**B** and **E**) and FVB (**C** and **F**) mice, 7 (**A–C**) and 60 (**D–F**) days after surgery. In sham-operated mice, using a rat anti-mouse CD34 antibody, we detected a predominant staining in glomeruli, with a faint staining in cortical peritubular capillaries (**A** and **D**). Because CD34 staining was identical in terms of distribution and intensity between B6D2F1 and FVB sham-operated mice, only one sham-operated kidney was shown at each time. CD34-positive cortical peritubular capillaries increased in remnant kidneys from both strains, 7 (compare **B** and **C** to **A**) and particularly 60 (compare **E** and **F** to **D**) days after surgery. The increase of capillary network was more prominent 60 days after surgery, particularly in FVB mice (compare **F** to **E**). Original magnifications,  $\times 400$ .

(Figure 3, A and D). In the remnant kidneys we recorded a modest increase in CD34 reactivity in this location on day 7 compared to sham-operated controls: this was more prominent in FVB/N *versus* C57BL6xDBA2/F1 mice (Figure 3, B and C). At day 60, the trend for increased immunostaining of peritubular capillaries became yet more prominent in the remnant kidneys of both strains, but was particularly striking in the FVB/N strain, especially in capillaries proximate to dilated tubules and microcysts (Figure 3, E and F). In addition, many of these vessels in the FVB/N strain appeared strikingly dilated

and often formed small lakes at the confluence of individual vessels. To quantify these differences, we counted, in peritubular areas of the cortex, the number of CD34-positive vessel sections and reported this to the number of tubular sections per microscopic field (Figure 4). In sham-operated animals, there was a slight, but not significant, increment of  $\sim 10\%$  during the period of observation. Moreover, the number of peritubular vessels was significantly higher in FVB/N than in C57BL6xDBA2/F1 sham-operated mice, but exclusively at day 7 after surgery. In nephrectomized mice, the num-

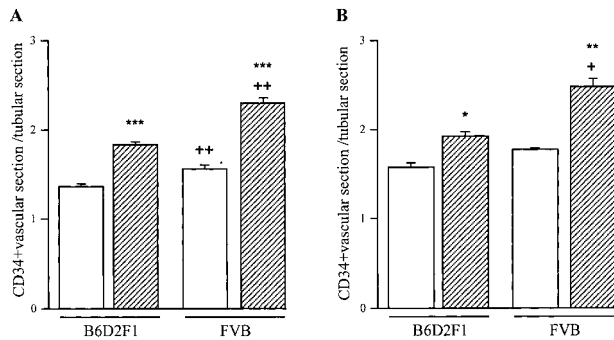


**Figure 4.** Quantification of cortical peritubular capillaries in sham-operated (open bars) and remnant (hatched bars) kidneys from B6D2F1 and FVB mice, 7 (A) and 60 (B) days after surgery. The number of CD34 longitudinal and transversal cross-sections was counted and factored for the number of tubules per field (original magnifications,  $\times 200$ ). The number of cortical peritubular vessels was significantly greater in remnant kidneys from nephrectomized mice, particularly in FVB strain, regardless of the experimental time point. Data are means  $\pm$  SEM. Analysis of variance, followed by Bonferroni test (Nx versus Sh mice: \*,  $P < 0.05$ , \*\*,  $P < 0.01$ , \*\*\*,  $P < 0.001$ ; FVB versus B6D2F1 mice: +,  $P < 0.05$ ; ++,  $P < 0.01$ ).

ber of vascular sections per tubular sections markedly increased in the cortex of remnant kidneys at days 7 and 60. At each time point, the increment was significantly higher in FVB/N strain as compared to C57BL6xDBA2/F1. The highest ratio of CD34-positive vascular/tubular sections were found at day 60 in FVB/N mice, when tubular lesions were apparent. Because the aim of the present study was to investigate the changes of the cortical peritubular microcirculation after nephron reduction, we did not formally analyze capillaries in glomeruli or medulla. However, CD34 immunostaining in these structures was intense and maintained throughout the course of the experiment in all groups.

In addition to analyzing CD34 reactivity in histological sections, we also used another marker of endothelia, the Tie-2 receptor tyrosine kinase. We have previously reported that immunohistochemical Tie-2 staining is prominent in the cortex of the developing cortical peritubular capillary plexus but is down-regulated with normal maturation.<sup>20</sup> In sham-operated kidneys we detected faint immunostaining restricted to glomerular capillaries, regardless the strain and the experimental time point. In contrast, in addition to the same glomerular pattern, we detected distinct Tie-2 immunostaining in cortical peritubular vessels of C57BL6xDBA2/F1 and FVB/N remnant kidneys 7 days after surgery (Figure 5, B and C). At day 60, the peritubular vessel staining persisted in FVB/N remnant kidneys (Figure 5F). At the last time point, the Tie-2-expressing vessels appeared dilated. Hence, this pattern was similar to that observed for CD34.

To obtain further information regarding the structure and, particularly, the function of the cortical peritubular vessels, we infused fluorescein isothiocyanate-dextran into the systemic circulation and visualized fluorescence in the kidney in histological sections of fixed kidneys. In sham-operated animals at 7 and 60 days, we observed prominent fluorescence in glomeruli and in vasa rectae: in contrast, there was only weak and inconstant signals from cortical peritubular vessels that appeared as thin lines adjacent to epithelia (Figure 6, A and D). A similar

pattern was observed in kidneys from control nonoperated animals (data not shown). In remnant kidneys of both mouse strains, a progressive increase in cortical peritubular fluorescence was evident on days 7 and 60 after surgery (Figure 6). The most marked changes were observed in FVB/N mice at 60 days after subtotal nephrectomy (Figure 6F) with prominent areas of fluorescence corresponding to the dilated vessels and vascular lakes that we had recorded with CD34 and Tie-2 immunohistochemistry.

### Endothelial and Epithelial Cell Proliferation

Collectively, the above results demonstrate a prominent and patent peritubular capillary network in the remnant kidney that is especially marked in the mouse strain which develops severe tubular lesions. To investigate whether endothelial cell proliferation contributes to this increment, we performed double immunostaining for CD34 and PCNA, a protein expressed in the nuclei of proliferating cells, and counted the number of double-labeled cells in the cortex (Table 2). In sham-operated animals, we recorded a low level of endothelial proliferation in the cortical peritubular microcirculation, except at day 7 in FVB/N mice, in which the number of CD34/PCNA double-stained cells was modestly increased. In contrast, the numbers of PCNA/CD34-positive peritubular endothelial cells increased dramatically at day 7 in both strains of nephrectomized mice, and was still higher at day 60. The increase was significantly more prominent (twofold) in FVB/N versus C57BL6xDBA2/F1 mice at both time points. In addition, we quantified PCNA-positive tubular epithelial cells (Table 2) and found that proliferation was rare in the sham-operated controls. In nephrectomized mice, the number of PCNA-labeled tubular cells increased significantly versus sham-controls at day 7 in both strains. At 60 days, this value decreased toward the control value in C57BL6xDBA2/F1 mice but remained elevated in the tubular lesions, which developed in FVB/N remnant kidneys. Therefore, the endothelial proliferation described here in the nephrectomized groups parallels the increased levels of CD34 on Western blot, the increased CD34 and Tie-2 immunostaining in cortical peritubular capillaries and the more prominent peritubular fluorescence visualized after administration of fluorescein isothiocyanate-dextran. Moreover, a positive correlation was found between tubular cell proliferation and endothelial cell proliferation in nephrectomized animals at both day 7 (linear regression:  $r^2 = 0.641$ ;  $P < 0.0001$ ) and 60 (linear regression:  $r^2 = 0.556$ ;  $P < 0.0001$ ).

### Expression of Vascular Growth Factors after Subtotal Nephrectomy

The next step was to attempt to identify the factors that might trigger capillary growth after nephron reduction. VEGF is considered an important stimulus to endothelial growth<sup>17</sup> and we therefore analyzed the expression of this factor in the experimental groups, comparing remnant kidneys and sham-operated organs at days 7 and

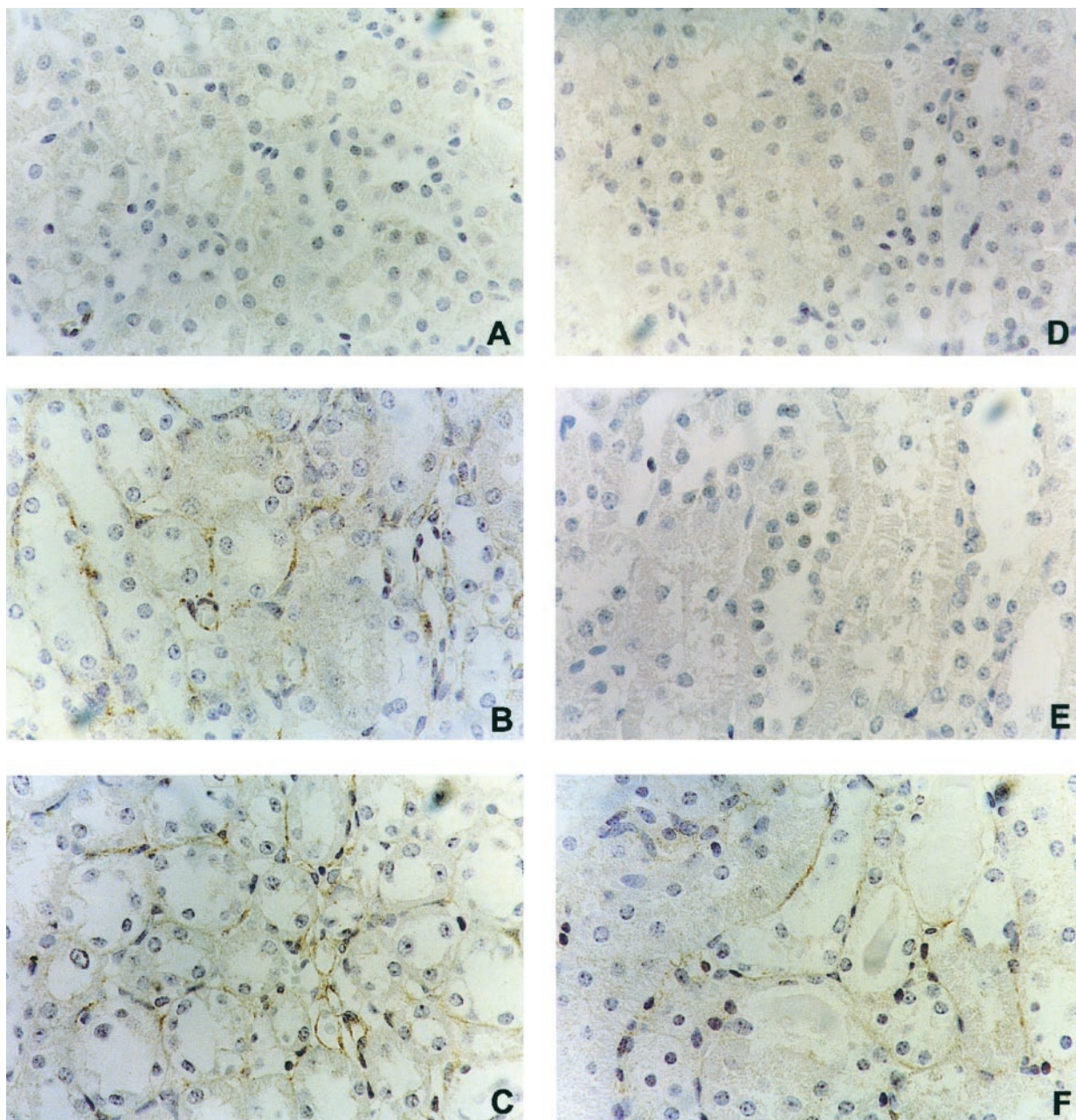


**Figure 5.** Immunohistochemical analysis of Tie-2 protein expression in cortex of sham-operated (**A** and **D**) and remnant (**B**, **C**, **E**, and **F**) kidneys from B6D2F1 (**B** and **E**) and FVB (**C** and **F**) mice, 7 (**A–C**) and 60 (**D–F**) days after surgery. In sham-operated mice, using a rabbit anti-human Tie-2 antibody, we detected a faint staining, restricted to glomerular capillaries. Because Tie-2 staining was identical in terms of distribution and intensity between B6D2F1 and FVB sham-operated mice, only one sham-operated kidney was shown at each time. Seven days after nephrectomy, we detected a marked peritubular capillary network in both strains (**B** and **C**), which persisted at day 60, but in FVB mice exclusively (compare **F** to **E**). Original magnifications,  $\times 400$ .

60. Immunohistochemistry, with or without microwave pretreatment, showed a diffuse VEGF staining in the kidneys of sham-operated mice (Figure 7, A and D, and data not shown), similar to that of control nonoperated animals, excluding any effect from sham-operation. The staining was more prominent in tubules using either method: proximal and distal convoluted tubules, collecting ducts, and loops of Henle all showed diffuse cytoplasmic staining. Glomerular staining was best seen using microwave-processed sections (data not shown): in these, VEGF protein could be detected in glomerular cells and Bowman's capsule. The distribution of VEGF

protein changed after nephron reduction, particularly in the FVB/N strain. Indeed, as compared to sham-operated animals, VEGF immunostaining showed a general decrease in proximal tubules and a marked increase in some distal tubules of remnant kidneys from FVB/N mice. As shown in Figure 7, these changes were more pronounced at day 60. A similar pattern was observed in remnant kidneys from C57BL6 $\times$ DBA2/F1 mice, but the changes were significantly less severe and were apparent exclusively at day 60. There were no differences of glomerular VEGF protein, in terms of amount and distribution, between the sham-operated and the nephrecto-



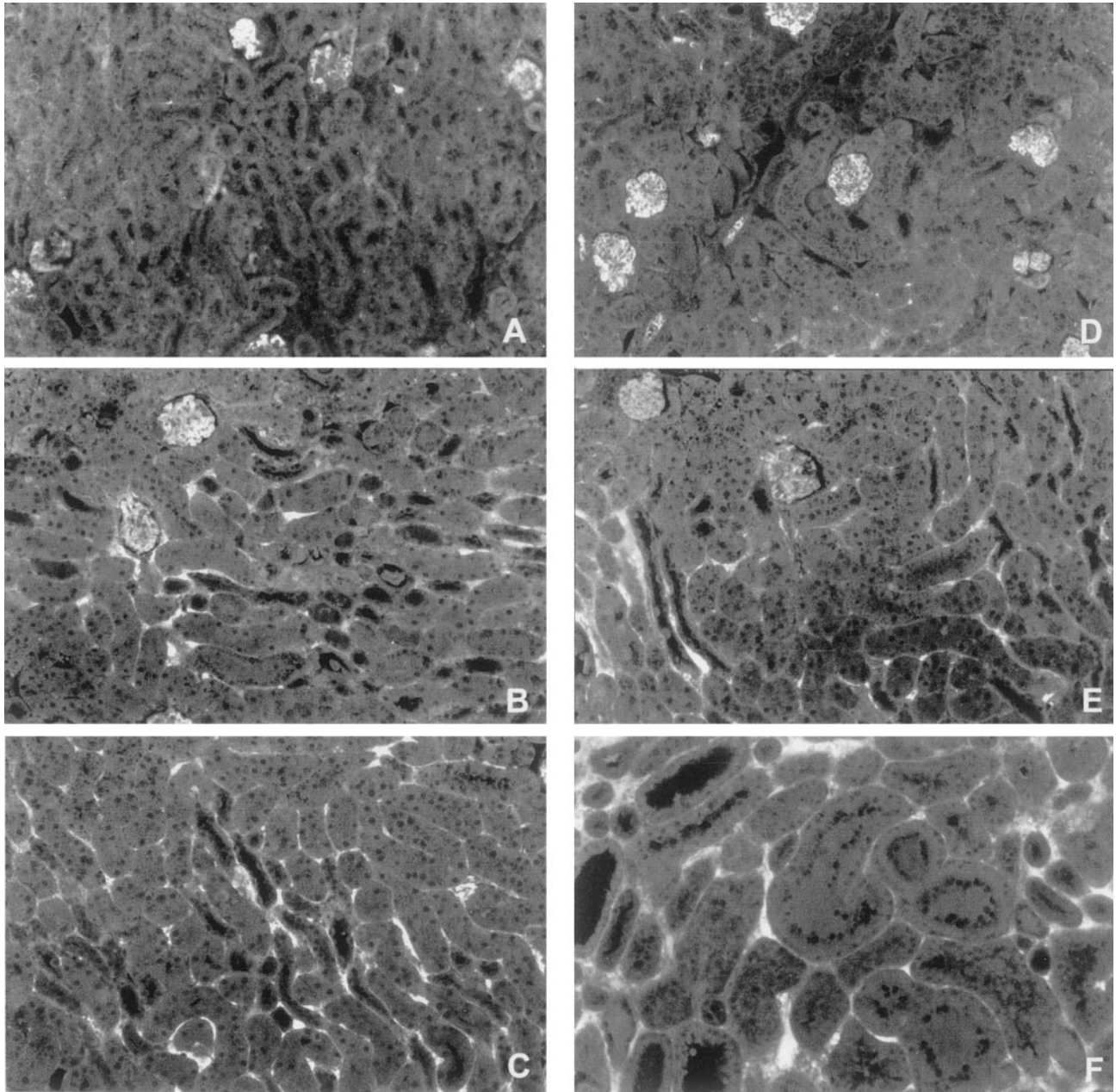


**Figure 6.** Fluorescein isothiocyanate-dextran microangiography of cortex of sham-operated (**A** and **D**) and FVB (**C** and **F**) mice, 7 (**A–C**) and 60 (**D–F**) days after surgery. In sham-operated mice, fluorescence was visualized exclusively in glomeruli. Because the intensity and the distribution of fluorescent dextran were identical between B6D2F1 and FVB sham-operated mice, only one sham-operated kidney was shown at each time. By contrast, fluorescence was detected in cortical peritubular capillaries of remnant kidneys from both strains at 7 (compare **B** and **C** to **A**) and 60 (compare **E** and **F** to **D**) days after surgery. At both experimental time points, fluorescence was more prominent in FVB strain (compare **C** to **B** and **F** to **E**). Original magnifications,  $\times 200$ .

mized mice, regardless the strain and the experimental time point.

To quantify the changes of VEGF protein expression after nephron reduction, we performed Western blot analysis. As shown in Figure 8, A and B, no differences were observed between the two sham-operated groups at any time of the study. VEGF protein levels markedly increased in remnant kidneys from nephrectomized mice at days 7 and 60, regardless of the strain used.

We next investigated whether the higher VEGF protein levels after nephron reduction correlated with mRNA lev-

els. Using Northern blots, we found no significant changes in VEGF mRNA at both day 7 and 60 (Figure 8, C and D). There were no differences in the patterns between the two strains regardless the experimental time point.

Finally, we analyzed the mRNA expression of other angiogenic factors (angiopoietin-1 and angiopoietin-2), known be expressed in kidney.<sup>20</sup> As observed for VEGF, Northern blot analysis showed that the angiopoietin-1 and angiopoietin-2 mRNA levels were similar in sham-operated and nephrectomized mice, at both 7 and 60

**Table 2.** Endothelial and Tubular Cell Proliferation

	PCNA/CD34 positive cells/field				PCNA positive tubular cells/field			
	B6D2F1		FVB		B6D2F1		FVB	
	Sh	Nx	Sh	Nx	Sh	Nx	Sh	Nx
Day 7								
Mean	0.007	0.122 <sup>†</sup>	0.033 <sup>§</sup>	0.202 <sup>‡§</sup>	0.9	22 <sup>*</sup>	1.3	21 <sup>†</sup>
SEM	0.002	0.025	0.008	0.031	0.3	7	0.2	2.6
Day 60								
Mean	0.005	0.047 <sup>†</sup>	0.006	0.104 <sup>‡§</sup>	0.6	3 <sup>*</sup>	1.8 <sup>§</sup>	23 <sup>†¶</sup>
SEM	0.003	0.013	0.002	0.022	0.2	0.8	0.4	4.7

Sh, sham-operated mice; Nx, subtotaly nephrectomized mice.

Data are mean ± SEM of six mice at each time. Analysis of variance: Nx versus Sh mice: \**P* < 0.05, †*P* < 0.01, ‡*P* < 0.001; FVB versus B6D2F1 mice: §*P* < 0.05; ¶*P* < 0.01.

days after surgery (data not shown). There were no differences between FVB/N and C57BL6xDBA2/F1 mice for both the molecules analyzed.

### Discussion

In the present study we have made three significant novel observations that illuminate the complex pathophysiology of chronic kidney damage after nephron reduction: 1) cortical peritubular capillaries grow, 2) VEGF expression is altered, and 3) the development of tubulo-interstitial disease is genetically determined. Interestingly, vascular changes are accentuated during the development of tubulo-interstitial lesions and positively correlate with tubular cell proliferation, suggesting an association between vessel growth and renal deterioration.

#### Peritubular Capillaries Grow after Nephron Reduction

Using a battery of techniques including microangiography, expression of CD34 and Tie-2 endothelial proteins, and PCNA/CD34 double immunostaining, we demonstrated that renal cortical peritubular capillaries increase and that their endothelial cells proliferate after nephron reduction in two strains of mice. Some of these responses correlated positively with tubular epithelial cell proliferation or were exaggerated in the presence of progressive tubulo-interstitial lesions in the FVB/N versus C57BL6xDBA2/F1 mice. Moreover, peritubular capillaries acquired an abnormal morphology after 75% nephrectomy: they appeared dilated and often formed small lakes at the confluence of individual vessels. Interestingly, a similar phenomenon has been reported in tumors<sup>24</sup> and in chronic inflammation,<sup>25</sup> two pathological conditions characterized by an important vascular rearrangement. Collectively, these findings demonstrate that surgical 75% nephron reduction in adult mice is associated with peritubular capillary growth rather than a reduction of capillary mass. We therefore speculate that blood perfusion to the tubulo-interstitium is most likely to be either normal or supranormal not only during compensatory renal growth but also during development of renal tubulo-interstitial lesions: however, further experiments that directly measure blood flow in this region will be necessary to prove this hypothesis.

Our conclusions regarding an expansion of renal cortical interstitial capillaries stand in contrast to other human and rat studies, alluded to in the Introduction, that report a decrease in microvessels in this location.<sup>12-14</sup> How can we explain such differences? It is possible to conceive that there are serial changes that occur in peritubular capillaries after nephron reduction that may be modulated by: 1) the species and age under study, 2) the extent and origin of nephron reduction, 3) the time after injury, and/or 4) the degree of fibrosis and/or tubular proliferation. With regard to our study, it is the first to examine the phenomenon in mice, rather than rats or humans; hence, the species may be important. Moreover, in the experimental model used, cell proliferation is known to be intense and to precede the development of renal lesions. In the present study, we were impressed by the observation that tubular epithelial proliferation with dilation and microcyst formation was prominent in FVB/N mice, and this strain had the more exaggerated vascular response. Furthermore, significant, but less marked, renal cortical microvascular changes occurred in the C57BL6xDBA2/F1 strain after nephron reduction, and also positively correlated with tubular cell proliferation: in the latter situation, interstitial fibrosis is insignificant. It may also be relevant that interstitial microvascular growth has also been reported in other kidney disorders in which epithelial proliferation is prominent, eg, adenocarcinoma<sup>26</sup> and autosomal dominant polycystic kidney disease.<sup>27</sup> In renal cell carcinoma, vessel density increases and correlates with tumor growth, stage, and grade as well as with the occurrence of metastasis.<sup>28</sup> Hence, there seems to be a functional positive correlation between endothelial and epithelial growth in the kidney and in other organs. The simplest explanation for this would be that a primary increase in epithelial growth triggers a supportive vascular response. One possibility would be that epithelial hypermetabolism would cause local tissue hypoxia, as has been hypothesized but not proven to occur in progressive renal disease,<sup>29</sup> and that this would stimulate new vessel growth by up-regulation of diverse growth factors, such as VEGF.<sup>30</sup> Whether hypoxia occurs in our mouse model remains to be established. However, we speculate that it is also possible that a primary increase in endothelial growth may be permissive for epithelial hyperproliferation. Indeed, therapies that block capillary growth, such as TNP-470<sup>31</sup> or endostatin,<sup>32</sup> sig-

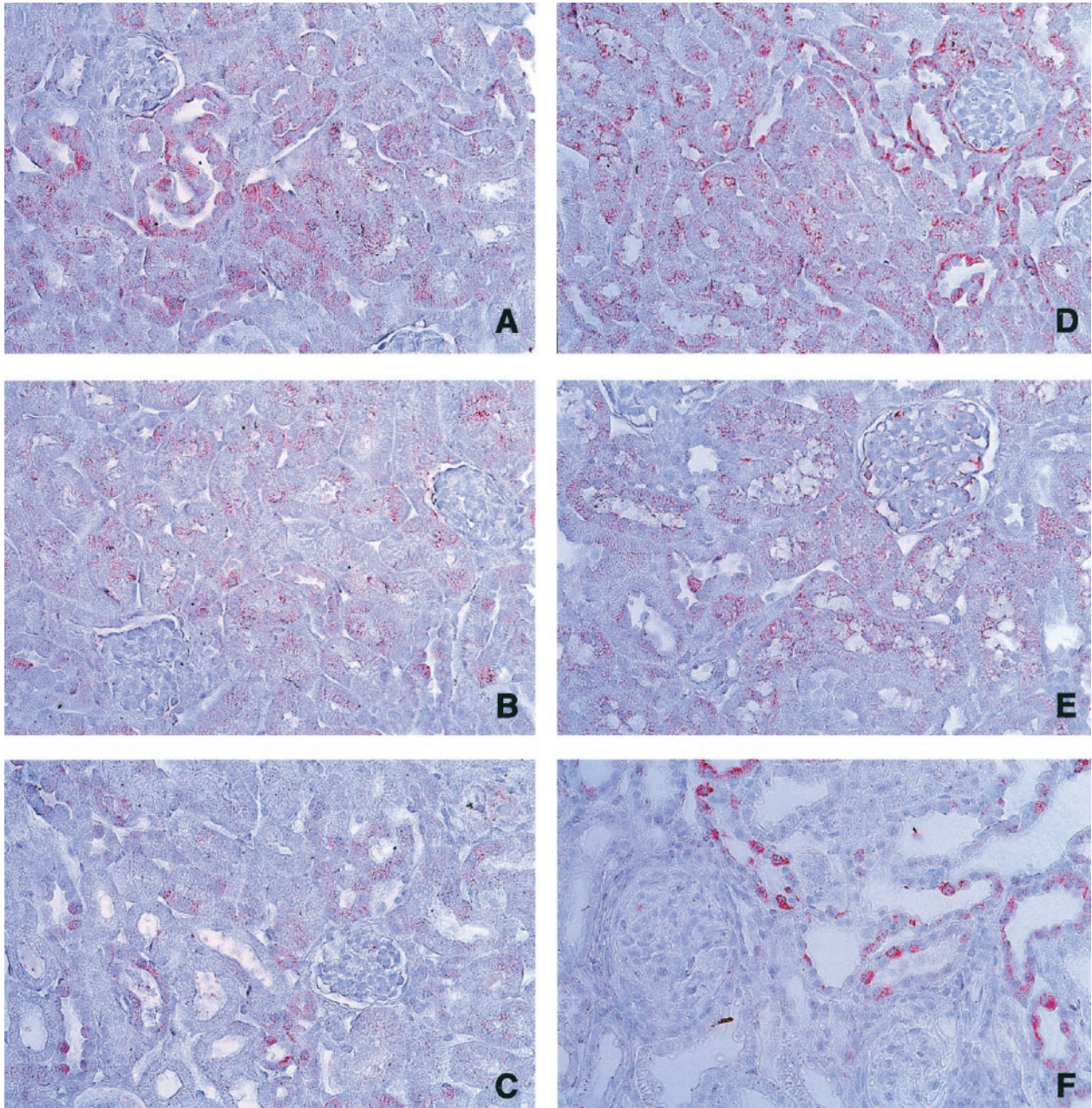


**Figure 7.** Immunohistochemical analysis of VEGF in sham-operated (**A** and **D**) and remnant (**B**, **C**, **E**, and **F**) kidneys from B6D2F1 (**B** and **E**) and FVB (**C** and **F**) mice, 7 (**A–C**) and 60 (**D–F**) days after surgery. In sham-operated mice, using a rabbit anti-human VEGF antibody, we detected a prominent staining in all of the tubules of the cortex (**A** and **D**). Because VEGF staining was identical in terms of distribution and intensity between B6D2F1 and FVB sham-operated mice, only one sham-operated kidney was shown at each time. After nephron reduction, VEGF staining decreased in proximal tubules, but increased in some distal tubules of remnant kidneys at both 7 (compare **B** and **C** to **A**) and 60 (compare **E** and **F** to **D**) days after surgery. The changes were greater in remnant kidneys from FVB mice, particularly at day 60 (compare **C** to **B** and **F** to **E**). Original magnifications,  $\times 400$ .

nificantly inhibit renal tumor epithelial proliferation and growth. Furthermore, capillary overgrowth also occurs in a wide spectrum of nonrenal disorders associated with epithelial cell proliferation, such as tumors,<sup>33</sup> cirrhosis,<sup>34</sup> retinopathies,<sup>35</sup> and psoriasis.<sup>36</sup> In all these disorders, anti-angiogenic therapies ameliorate the evolution of the disease.<sup>37</sup> In the future, the primacy of the vascular or epithelial response could be ascertained in the FVB/N and C57BL6xDBA2/F1 mice subjected to nephron reduction by using therapies that inhibit the endothelial or tubular epithelial cell proliferation of either lineage.

### *VEGF Expression Is Altered after Nephron Reduction*

In the present study, we provide evidence that, in remnant mouse kidneys, VEGF protein changed: in Western blots of lysates of whole kidneys, levels of VEGF significantly increased during both compensatory and pathological responses. However, when we analyzed the detailed tissue distribution by immunohistochemistry, a more complex picture emerged with an increase of im-

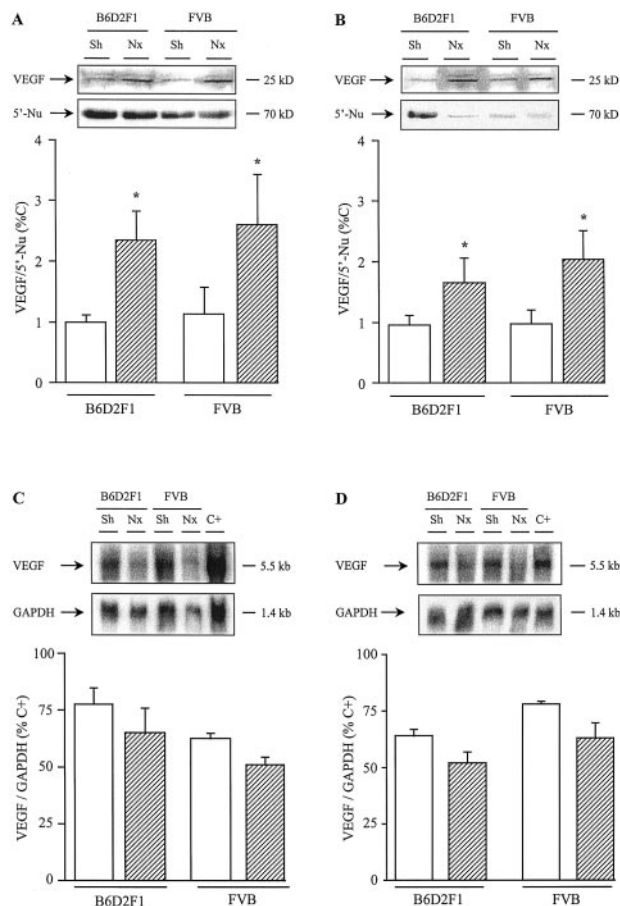


**Figure 8.** Western blot (A and B) and Northern blot (C and D) of VEGF in sham-operated (open bars) and remnant (hatched bars) kidneys from B6D2F1 and FVB mice, 7 (A and C) and 60 (B and D) days after surgery. A and B: Compared to sham-operated mice, VEGF protein increased significantly after nephron reduction in both strains regardless of the experimental time point. C and D: VEGF mRNA did not change significantly in remnant kidneys compared to a sham-operated one, regardless of the strain and the experimental time point. Total heart mRNA was used as positive control (C<sup>+</sup>). Blots are representative samples of six animals from each group. Data are means ± SEM. Analysis of variance, followed by Bonferroni test (Nx versus Sh mice; \*, *P* < 0.05).

munostaining in cortical distal-type tubules and an apparent decrease in proximal-type tubules. VEGF has been shown to bind to renal peritubular capillaries.<sup>38</sup> Interestingly, endothelial cell proliferation significantly increased in this location in our study. Hence, we speculate that, after subtotal nephrectomy, some VEGF may become sequestered in the interstitium and that this protein may be detected by Western blot but not by the immunohistochemical techniques used in this study. Certainly, the specific procedures used to prepare tissue sections may affect detection of VEGF; for example, we have observed that microwaving enhances the glomerular staining of this protein (data not shown).

Renal VEGF levels, as assessed by the intensity of immunostaining, have previously been found to increase in diverse chronic renal diseases including glomerulonephritis,<sup>39,40</sup> diabetes,<sup>41</sup> and chronic vascular transplant rejection.<sup>40</sup> Functional experiments have implicated VEGF in glomerulogenesis as well as in capillary repair after experimental glomerular injury.<sup>42</sup> In addition, in isch-

emic kidneys, Kanellis and colleagues<sup>43</sup> showed a prominent shift of cytoplasmic VEGF to the basolateral membrane of tubular cells, without any changes in total VEGF protein levels. However, ours is the first study to assess serial changes in defined experimental model of compensatory and pathological responses to nephron reduction. At present we can only speculate as to the conditions that up-regulate VEGF protein levels as observed in the current study. Two, of many, possibilities include epidermal growth factor, a molecule that is known to be up-regulated after nephron reduction<sup>44</sup> and that can stimulate VEGF production and secretion,<sup>17</sup> as well as hypoxia, which has been postulated to exist in chronic nephropathies<sup>29</sup> and that has been proven to up-regulate VEGF.<sup>30</sup> In the future, the measurement of oxygen tension in remaining nephrons and/or the use of the dominant-negative transgenic strategy to down-regulate epidermal growth factor receptor activation<sup>9</sup> could be used to investigate these hypotheses.

A number of angiogenic growth factors are synthesized within the kidney and the expression of several, such as fibroblastic growth factor, platelet-derived growth factor, and endothelin, are up-regulated in several experimental and human nephropathies.<sup>44</sup> In the current study, we found that angiotensin-1 and -2 mRNA were not up-regulated after nephron reduction. Further studies using Western blot and immunohistochemistry may be informative in the future, especially because the increases in VEGF protein on Western blot occurred despite no change in levels of transcripts as judged by Northern blot.

### *The Response to Nephron Reduction Is Genetically Determined*

We discovered a different susceptibility between two mice strains with regard to development of progressive renal lesions after subtotal nephrectomy, even though they both underwent a period of compensatory growth. After a 75% reduction in renal mass, FVB/N mice developed pathological tubular dilation, interstitial fibrosis, and glomerulosclerosis, whereas C57BL6xDBA2/F1 mice, as other mouse strains previously described (eg, C57BL6),<sup>45</sup> were resistant to renal deterioration. This establishes the mouse as a model for progressive tubulo-interstitial renal lesions, an important observation because this species can be genetically engineered with a view to assessing which genes modulate the course of renal disease.<sup>9</sup> We are aware of only one other mouse strain, the 129/Sv, which develops renal lesions after subtotal nephrectomy,<sup>46</sup> but, in contrast to the FVB/N strain, glomerular lesions were prominent as compared to tubulo-interstitial ones. Similarly, Esposito and colleagues<sup>47</sup> reported that unilateral nephrectomy induced glomerulosclerosis in ragged oligosyndactyly pintail (ROP), but not in C57BL6 mice.<sup>47</sup> However, tubulo-interstitial lesions did not develop in this model in either strain. In the future, it will be also interesting to explore the genetic bases of the different susceptibilities between the FVB/N and C57BL6xDBA2/F1 strains to discover key genes that enhance, or protect

animals against progressive renal tubulo-interstitial disease. Whether genetic factors influence vessel remodeling and/or growth has been little investigated. Thurston and colleagues<sup>25</sup> showed that vascular remodeling is qualitatively different in two strains of mice, the C57BL6 and the C3H, with chronic airway inflammation induced by *Mycoplasma pulmonis* infection. Similarly genetic background has been shown to influence vessel formation during development in mice in which tissue factor was inactivated by homologous recombination.<sup>48</sup> The factor(s) that could be involved directly or indirectly in angiogenesis and be genetically determined in FVB/N mice remain(s) to be elucidated.

### Conclusions

Using the different susceptibility of two mice strains to develop renal lesions after subtotal nephrectomy, we showed that peritubular capillary network increased after nephron reduction and that this increment correlated to the rate of cell proliferation and to the severity of tubular lesions. Further work, to elucidate the effects of anti-angiogenesis agents in these models and to measure oxygen tensions in the diseased tubulo-interstitium, are likely to give further insight into the pathophysiology of renal deterioration after nephron reduction.

### Acknowledgments

We thank B. Kaissling for anti-5'-nucleotidase antibody and E. Solito for GAPDH probe.

### References

1. Hostetter TH: Progression of renal disease and renal hypertrophy. *Annu Rev Physiol* 1995, 57:263-278
2. Olivetti G, Anversa P, Rigamonti W, Vitali-Mazza L, Loud AV: Morphometry of the renal corpuscle during normal postnatal growth and compensatory hypertrophy. A light microscope study. *J Cell Biol* 1977, 75:573-585
3. Terzi F, Ticozzi C, Burtin M, Motel V, Beaufils H, Laouari D, Assael BM, Kleinknecht C: Subtotal but not unilateral nephrectomy induces hyperplasia and protooncogene expression. *Am J Physiol* 1995, 268:F793-F801
4. Kliem V, Johnson RJ, Alpers CE, Yoshimura A, Couser WG, Koch KM, Floege J: Mechanisms involved in the pathogenesis of tubulointerstitial fibrosis in 5/6-nephrectomized rats. *Kidney Int* 1996, 49:666-678
5. Terzi F, Burtin M, Hekmati M, Jouanneau C, Beaufils H, Friedlander G: Sodium restriction decreases AP-1 activation after nephron reduction in the rat: role in the progression of renal lesions. *Exp Nephrol* 2000, 8:104-114
6. Ishidoya S, Morrissey J, McCracken R, Reyes A, Klahr S: Angiotensin II receptor antagonist ameliorates renal tubulointerstitial fibrosis caused by unilateral ureteral obstruction. *Kidney Int* 1995, 47:1285-1294
7. Johnson RJ, Raines EW, Floege J, Yoshimura A, Pritzl P, Alpers C, Ross R: Inhibition of mesangial cell proliferation and matrix expansion in glomerulonephritis in the rat by antibody to platelet-derived growth factor. *J Exp Med* 1992, 175:1413-1416
8. Kashihara N, Maeshima Y, Makino H: Therapeutic intervention in glomerulonephritis by oligonucleotides. *Exp Nephrol* 1997, 5:126-131
9. Terzi F, Burtin M, Hekmati M, Federici P, Grimber G, Briand P, Friedlander G: Targeted expression of a dominant-negative EGF-R in

- the kidney reduces tubulo-interstitial lesions after renal injury. *J Clin Invest* 2000, 106:225-234
10. Nagata M, Scharer K, Kriz W: Glomerular damage after uninephrectomy in young rats. I. Hypertrophy and distortion of capillary architecture. *Kidney Int* 1992, 42:136-147
11. Kitamura H, Shimizu A, Masuda Y, Ishizaki M, Sugisaki Y, Yamanaka N: Apoptosis in glomerular endothelial cells during the development of glomerulosclerosis in the remnant-kidney model. *Exp Nephrol* 1998, 6:328-336
12. Ohashi R, Kitamura H, Yamanaka N: Peritubular capillary injury during the progression of experimental glomerulonephritis in rats. *J Am Soc Nephrol* 2000, 11:47-56
13. Seron D, Alexopoulos E, Raftery MJ, Hartley B, Cameron JS: Number of interstitial capillary cross-sections assessed by monoclonal antibodies: relation to interstitial damage. *Nephrol Dial Transplant* 1990, 5:889-893
14. Bohle A, Mackensen-Haen S, Wehrmann M: Significance of postglomerular capillaries in the pathogenesis of chronic renal failure. *Kidney Blood Press Res* 1996, 19:191-195
15. Konda R, Sato H, Sakai K, Sato M, Orikasa S, Kimura N: Expression of platelet-derived endothelial cell growth factor and its potential role in up-regulation of angiogenesis in scarred kidneys secondary to urinary tract diseases. *Am J Pathol* 1999, 155:1587-1597
16. Carmeliet P: Mechanisms of angiogenesis and arteriogenesis. *Nat Med* 2000, 6:389-395
17. Ferrara N: Role of vascular endothelial growth factor in the regulation of angiogenesis. *Kidney Int* 1999, 56:794-814
18. Kitamoto Y, Tokunaga H, Tomita K: Vascular endothelial growth factor is an essential molecule for mouse kidney development: glomerulogenesis and nephrogenesis. *J Clin Invest* 1997, 99:2351-2357
19. Simon M, Grone HJ, Jöhren O, Kullmer J, Plate KH, Risau W, Fuchs E: Expression of vascular endothelial growth factor and its receptors in human renal ontogenesis and in adult kidney. *Am J Physiol* 1995, 268:F240-F250
20. Yuan HT, Suri C, Yancopoulos GD, Woolf AS: Expression of angiopoietin-1, angiopoietin-2, and the Tie-2 receptor tyrosine kinase during mouse kidney maturation. *J Am Soc Nephrol* 1999, 10:1722-1736
21. Terzi F, Henrion D, Colucci-Guyon E, Federici P, Babinet C, Levy BI, Briand P, Friedlander G: Reduction of renal mass is lethal in mice lacking vimentin. Role of endothelin-nitric oxide imbalance. *J Clin Invest* 1997, 100:1520-1528
22. Terzi F, Beaufils H, Laouari D, Burtin M, Kleinknecht C: Renal effect of anti-hypertensive drugs depends on sodium diet in the excision remnant kidney model. *Kidney Int* 1992, 42:354-363
23. Laouari D, Friedlander G, Burtin M, Silve C, Dechaux M, Garabedian M, Kleinknecht C: Subtotal nephrectomy alters tubular function: effect of phosphorus restriction. *Kidney Int* 1997, 52:1550-1560
24. Helmlinger G, Yuan F, Dellian M, Jain RK: Interstitial pH and pO<sub>2</sub> gradients in solid tumors in vivo: high-resolution measurements reveal a lack of correlation. *Nat Med* 1997, 3:177-182
25. Thurston G, Murphy TJ, Baluk P, Lindsey JR, McDonald DM: Angiogenesis in mice with chronic airway inflammation: strain-dependent differences. *Am J Pathol* 1998, 153:1099-1112
26. Brown LF, Berse B, Jackman RW, Tognazzi K, Manseau EJ, Dvorak HF, Senger DR: Increased expression of vascular permeability factor (vascular endothelial growth factor) and its receptors in kidney and bladder carcinomas. *Am J Pathol* 1993, 143:1255-1262
27. Bello-Reuss E, Rajaraman S: Angiogenesis in autosomal dominant polycystic kidney disease. *J Am Soc Nephrol* 2000, 11:A2023
28. Strohmeier D: Pathophysiology of tumor angiogenesis and its relevance in renal cell cancer. *Anticancer Res* 1999, 19:1557-1561
29. Fine LG, Bandyopadhyay D, Norman JT: Is there a common mechanism for the progression of different types of renal diseases other than proteinuria? Towards the unifying theme of chronic hypoxia. *Kidney Int* 2000, 57(Suppl 75):S22-S26
30. Shweiki D, Itin A, Soffer D, Keshet E: Vascular endothelial growth factor induced by hypoxia may mediate hypoxia-initiated angiogenesis. *Nature* 1992, 359:843-845
31. Morita T, Shinohara N, Tokue A: Antitumor effect of a synthetic analogue of fumagillin on murine renal carcinoma. *Br J Urol* 1994, 74:416-421
32. Dhanabal M, Ramchandran R, Volk R, Stillman IE, Lombardo M, Iruela-Arispe ML, Simons M, Sukhatme VP: Endostatin: yeast produc-

- tion, mutants, and antitumor effect in renal cell carcinoma. *Cancer Res* 1999, 59:189–197
33. Folkman J, Watson K, Ingber D, Hanahan D: Induction of angiogenesis during the transition from hyperplasia to neoplasia. *Nature* 1989, 339:58–61
  34. Rosmorduc O, Wendum D, Corpechot C, Galy B, Sebbagh N, Raleigh J, Housset C, Poupon R: Hepatocellular hypoxia-induced vascular endothelial growth factor expression and angiogenesis in experimental biliary cirrhosis. *Am J Pathol* 1999, 155:1065–1073
  35. Aiello LP, Avery RL, Arrigg PG, Keyt BA, Jampel HD, Shah ST, Pasquale LR, Thieme H, Iwamoto MA, Park JE, Nguyen HU, Aiello LM, Ferrara N, King GL: Vascular endothelial growth factor in ocular fluid of patients with diabetic retinopathy and other retinal disorders. *N Engl J Med* 1994, 331:1480–1487
  36. Creamer D, Allen MH, Sousa A, Poston R, Barker JN: Localization of endothelial proliferation and microvascular expansion in active plaque psoriasis. *Br J Dermatol* 1997, 136:859–865
  37. Griffioen AW, Molema G: Angiogenesis: potentials for pharmacologic intervention in the treatment of cancer, cardiovascular diseases, and chronic inflammation. *Pharmacol Rev* 2000, 52:237–268
  38. Simon M, Rockl W, Hornig C, Grone EF, Theis H, Weich HA, Fuchs E, Yayon A, Grone HJ: Receptors of vascular endothelial growth factor/vascular permeability factor (VEGF/VPF) in fetal and adult human kidney: localization and [<sup>125</sup>I]VEGF binding sites. *J Am Soc Nephrol* 1998, 9:1032–1044
  39. Shulman K, Rosen S, Tognazzi K, Manseau EJ, Brown LF: Expression of vascular permeability factor (VPF/VEGF) is altered in many glomerular diseases. *J Am Soc Nephrol* 1996, 7:661–666
  40. Grone HJ, Simon M, Grone EF: Expression of vascular endothelial growth factor in renal vascular disease and renal allografts. *J Pathol* 1995, 177:259–267
  41. Williams B: A potential role for angiotensin II-induced vascular endothelial growth factor expression in the pathogenesis of diabetic nephropathy? *Miner Electrolyte Metab* 1998, 24:400–405
  42. Ostendorf T, Kunter U, Eitner F, Loos A, Regele H, Kerjaschki D, Henninger DD, Janjic N, Floege J: VEGF(165) mediates glomerular endothelial repair. *J Clin Invest* 1999, 104:913–923
  43. Kanellis J, Mudge SJ, Fraser S, Katerelos M, Power DA: Redistribution of cytoplasmic VEGF to the basolateral aspect of renal tubular cells in ischemia-reperfusion injury. *Kidney Int* 2000, 57:2445–2456
  44. Terzi F, Burtin M, Friedlander G: Early molecular mechanisms in the progression of renal failure: role of growth factors and protooncogenes. *Kidney Int* 1998, 53 (Suppl 65):S68–S73
  45. Kren S, Hostetter TH: The course of the remnant kidney model in mice. *Kidney Int* 1999, 56:333–337
  46. Megyesi J, Price PM, Tamayo E, Safirstein RL: The lack of a functional p21(WAF1/CIP1) gene ameliorates progression to chronic renal failure. *Proc Natl Acad Sci USA* 1999, 96:10830–10835
  47. Esposito C, He CJ, Striker GE, Zalups RK, Striker LJ: Nature and severity of the glomerular response to nephron reduction is strain-dependent in mice. *Am J Pathol* 1999, 154:891–897
  48. Toomey JR, Kratzer KE, Lasky NM, Broze Jr GJ: Effect of tissue factor deficiency on mouse and tumor development. *Proc Natl Acad Sci USA* 1997, 94:6922–6926